

*Electronic supplement Information (ESI)*

**A Label-free Multiplex Electrochemical Biosensor for Detection of Three Breast Cancer Biomarker Proteins Employing Dye/Metal Ions-loaded and Antibodies-Conjugated Polyethyleneimine-Gold Nanoparticles**

Kulrisa Kuntamung<sup>a,b</sup>, Jaron Jakmune<sup>a,c,d,e</sup>, Kontad Ounnunkad<sup>a,c,d,e\*</sup>

<sup>a</sup>*Department of Chemistry, Faculty of Science, Chiang Mai University, Chiang Mai 50200, Thailand*

<sup>b</sup>*The Graduate School, Chiang Mai University, Chiang Mai 50200, Thailand*

<sup>c</sup>*Center of Excellence for Innovation in Chemistry, Faculty of Science, Chiang Mai University, Chiang Mai, 50200, Thailand*

<sup>d</sup>*Research Center on Chemistry for Development of Health Promoting Products from Northern Resources, Chiang Mai University, Chiang Mai, 50200, Thailand*

<sup>e</sup>*Center of Excellence in Materials Science and Technology, Chiang Mai University, Chiang Mai 50200, Thailand*

\*Corresponding author

Emails: [suriyacmu@yahoo.com](mailto:suriyacmu@yahoo.com), [kontad.ounnunkad@cmu.ac.th](mailto:kontad.ounnunkad@cmu.ac.th)

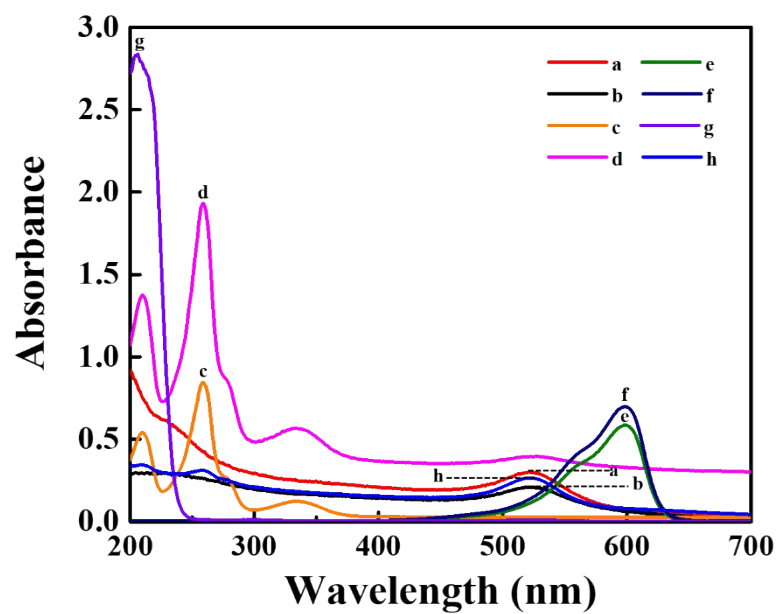


**Fig. S1** UV-Visible absorption spectra of (a) PEI-AuNPs, (b) antibody-PEI-AuNPs, (c) AQ, (d) AQ-antibody-PEI-AuNPs, (e) TH, (f) TH-antibody-PEI-AuNPs, (g) Ag<sup>+</sup>, and (h) Ag<sup>+</sup>-antibody-PEI-AuNPs.

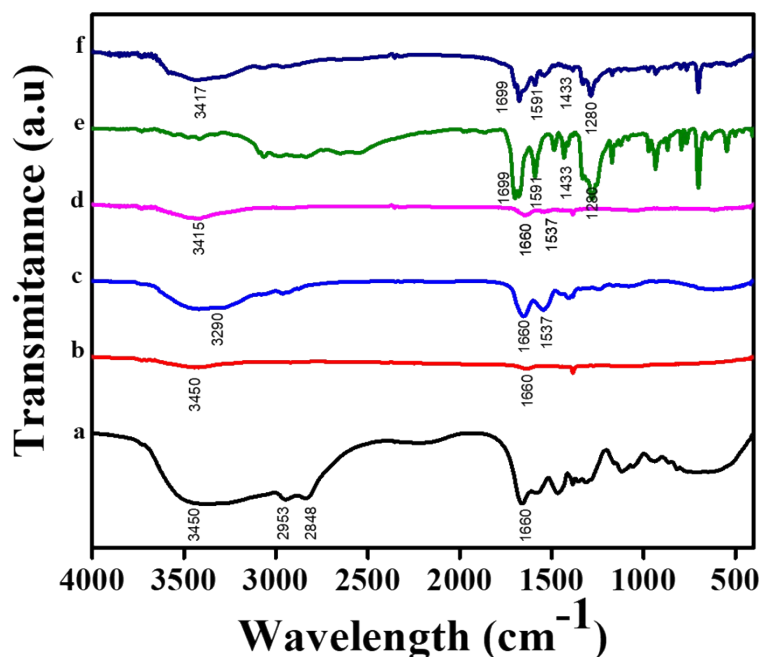


**Fig. S2** FT-IR spectra of PEI (a), PEI-AuNPs (b), antibody (c), antibody-PEI-AuNPs (d), AQ (e), and AQ-antibody-PEI-AuNPs (d).

The FT-IR spectra of PEI (a) shows characteristic peaks at 3,450 and 1,660  $\text{cm}^{-1}$ , which can be assigned to stretching and bending vibrations of N-H and  $-\text{NH}_2$ , respectively. The peaks at 2953 and 2848  $\text{cm}^{-1}$  can be assigned to C-H stretching. The PEI-functionalized AuNPs exhibit the small characteristic absorption peaks of amine groups located at 3,450 and 1,660  $\text{cm}^{-1}$  (b), confirming the presence of PEI in the PEI-AuNPs product. After the immobilization of antibody onto the surface of PEI-AuNPs, the absorption peak at 1660  $\text{cm}^{-1}$  and 1537  $\text{cm}^{-1}$  can indicate C=O, C-N stretching or N-H bending, which are associated with the antibody. Subsequently, when AQ is attached to antibodies-conjugated PEI-AuNPs, the observable peak at 1699  $\text{cm}^{-1}$  is the C=O stretching vibration peak of AQ. Moreover, the feature bands at 1591  $\text{cm}^{-1}$ , 1433  $\text{cm}^{-1}$ , and 1280  $\text{cm}^{-1}$  indicates the skeletal structure of aromatic ring, which is consistent with that of AQ (e). In addition, the peak at 3417  $\text{cm}^{-1}$  belongs to N-H, C-H stretching, and OH bonding (f), which correspond to those of PEI, antibodies, and AQ (superimposing broad peak). It is plausible that AQ and antibodies has been successfully attached on PEI-AuNPs.

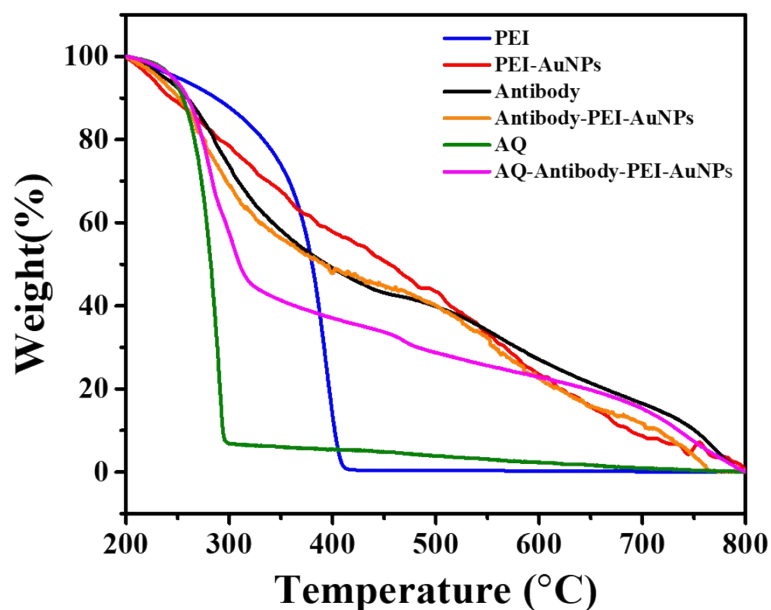


**Fig. S3** TGA curves heating from 25 to 800 °C ( $10\text{ °C min}^{-1}$ ) under a flow of  $\text{N}_2$ .

As seen in Fig. S3, PEI is completely degraded at *ca.* 420 °C while AQ is completely degraded at *ca.* 290 °C. PEI-AuNPs degrade continuously over the range 200-800 °C and antibody degrade with three steps of 200-450, 450-700, and 700-800 °C. Antibody-conjugated PEI-coated AuNPs present the three-step degradation profile similar to that of antibody, indicating successful attachment of antibody onto PEI-AuNPs. The final product, AQ/antibody-conjugated PEI-coated AuNPs, shows the deep first step degradation close to the degradation temperature of AQ, indicating the attachment of AQ onto antibody-conjugated PEI-AuNPs. Moreover, the second step degradation of the final product is similar to that of antibody, suggesting presence of antibody in the PEI-AuNPs. Since the PEI-AuNPs is degraded over wide range, the degradation profile of PEI-AuNPs is superimposed and might have no contribution to the character of degradation profiles of the products, antibody-PEI-AuNPs and AQ-antibody-PEI-AuNPs. This result agrees well with that of the FT-IR experiment.

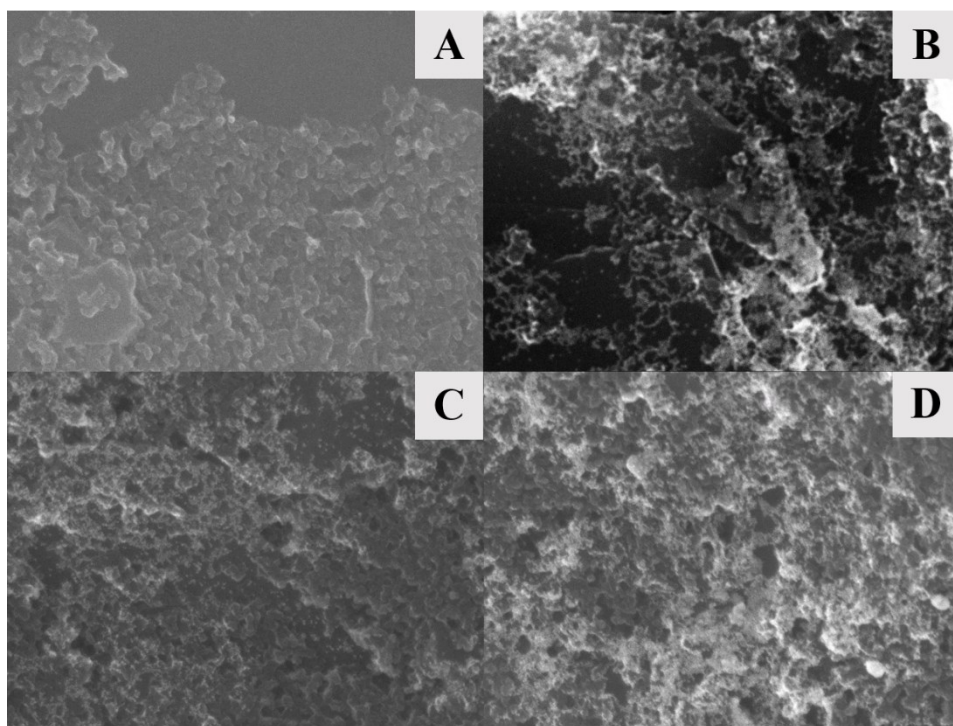


**Fig. S4** SEM images of (A) bare SPCE and (B) anti-MUC1-AQ-PEI-AuNPs-, (C) anti-CA15-3-TH-PEI-AuNPs-, and (D) anti-HER2-Ag-PEI-AuNPs-modified SPCEs.

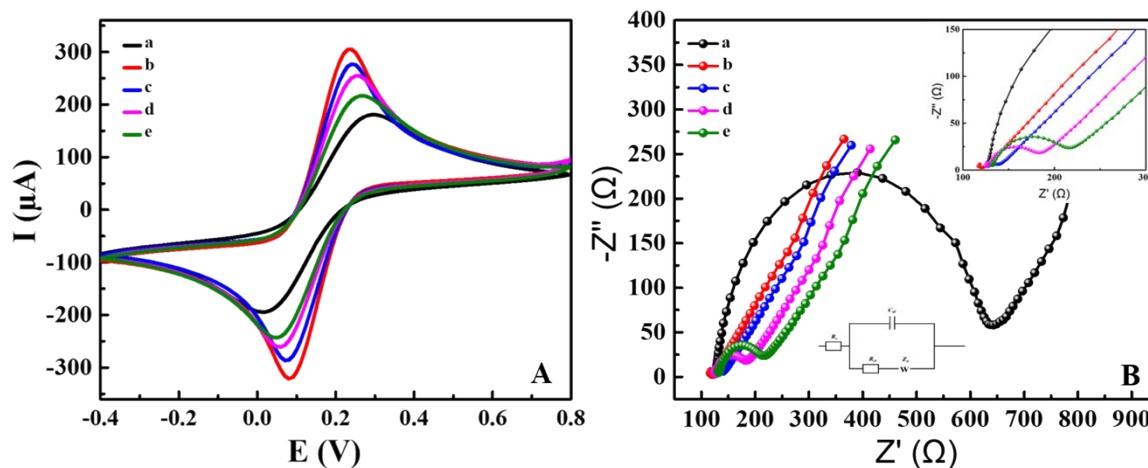


**Fig. S5** The signal change of CV curves (A) and EIS spectra (B) during the fabrication process of the immunosensor, in 0.010 M PBS (pH 7.4) solution containing 5.0 mM  $[\text{Fe}(\text{CN})_6]^{3-/4-}$  at a scan rate of 50 mV/s for (a) bare SPCE, (b) PEI-AuNPs modified SPCE, (c) antibodies-PEI-AuNPs modified SPCE, and (d) antibodies-PEI-AuNPs modified SPCE after blocked with 0.05% BSA and (e) after incubation with antigens. (the inset shows the magnified area of low impedance and the equivalent circuit model)

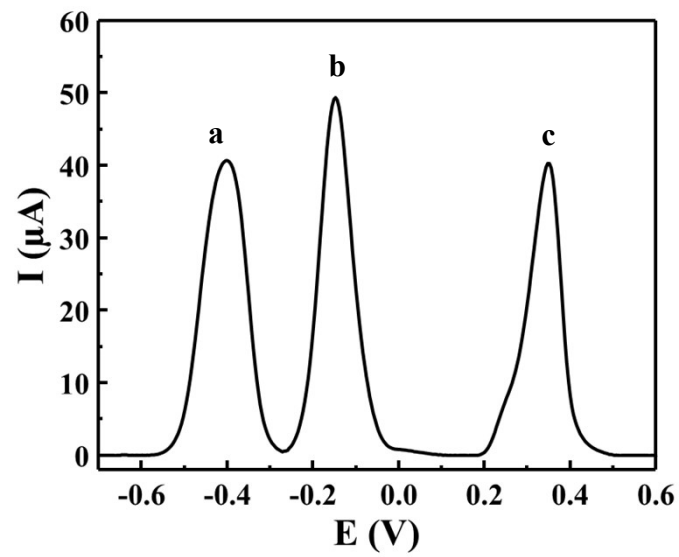


**Fig. S6** Typical SWV signals of AQ-anti-MUC1-PEI-AuNPs (a), TH-anti-CA15-3-PEI-AuNPs (b), and  $\text{Ag}^+$ -anti-HER2-PEI-AuNPs (c)

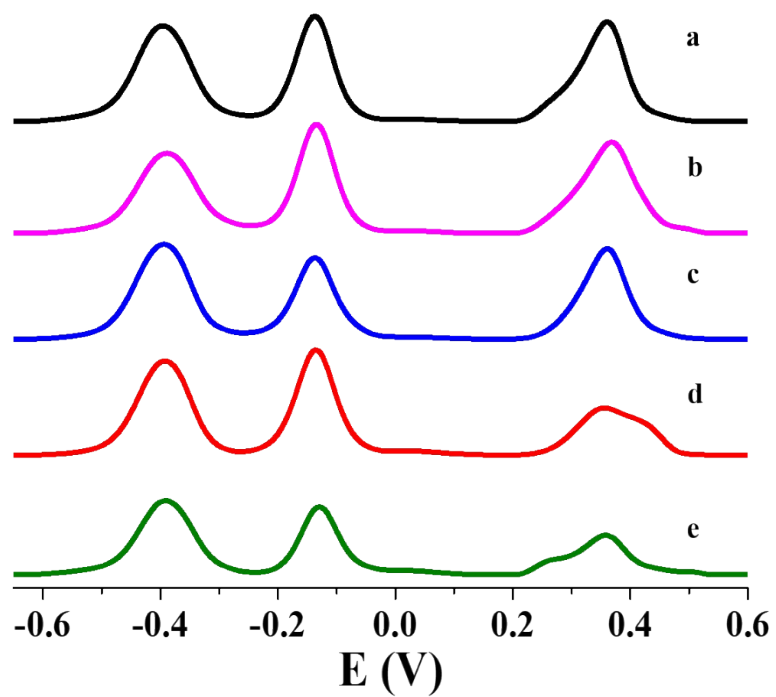


**Fig. S7** SWV measurements for the investigation of cross-reactivity; blank (a) single analyte of 25 ng mL<sup>-1</sup> MUC1 (b), 25 U mL<sup>-1</sup> CA15-3 (c), and 25 ng mL<sup>-1</sup> HER2 (d); the analyte mixture containing 25 ng mL<sup>-1</sup> MUC1, 25 U mL<sup>-1</sup> CA15-3 and 25 ng mL<sup>-1</sup> HER2 (e).



**Table S1** Comparison of the analytical performances of electrochemical immunosensors

Biomarker	Electrode modification	Detection	Linear range	LOD	Ref.
CA 15-3, HER2	AP-Anti1/Anti2/AuNPs/bi-SPCE (sandwich-type immunosensor)	LSV	CA 15-3: 0-70 U mL <sup>-1</sup> HER2: 0-50 ng mL <sup>-1</sup>	CA 15-3: 5.0 U mL <sup>-1</sup> HER2: 2.9 ng mL <sup>-1</sup>	[1]
HER2	Anti-HER2/Fe <sub>3</sub> O <sub>4</sub> NPs (label-free immunosensor)	DPV	0.01-10 ng mL <sup>-1</sup> and 10-100 ng mL <sup>-1</sup>	9.95x10 <sup>-4</sup> ng mL <sup>-1</sup>	[2]
MUC1	AuNPs-graphite SPE by EIS AuNPs-gold SPE by DPV (label-free immunosensor)	EIS DPV	EIS: 2.5-15 ng mL <sup>-1</sup> DPV: 0-10 ng mL <sup>-1</sup>	EIS: 3.6 ng mL <sup>-1</sup> DPV: 0.95 ng mL <sup>-1</sup>	[3]
MUC1	APT/SA/AuNPs-GO-PEDOT/FTO (label-free immunosensor)	DPV	0.1 fg mL <sup>-1</sup> -1 µg mL <sup>-1</sup>	1 x10 <sup>-6</sup> ng mL <sup>-1</sup>	[4]
CEA, CA15-3, CA125	Anti/MB-Chi/GR/ITO (label-free immunosensor)	LSV	CA15-3: 0.0001-0.0025 U mL <sup>-1</sup> and 0.0025-0.1 U mL <sup>-1</sup>	CA15-3: 0.00004 U mL <sup>-1</sup>	[5]
MUC1, CA15-3, HER2	AQ/Anti-MUC1/PEI-AuNPs/SPCE TH/Anti-CA15-3/PEI-AuNPs/SPCE Ag <sup>+</sup> /Anti-HER2/PEI-AuNPs/SPCE	SWV	MUC1: 0.10-100 ng mL <sup>-1</sup> CA15-3: 0.10-100 U mL <sup>-1</sup> HER2: 0.10-100 ng mL <sup>-1</sup>	MUC1: 0.53 ng mL <sup>-1</sup> CA15-3: 0.21 U mL <sup>-1</sup> HER2: 0.50 ng mL <sup>-1</sup>	This work

Alkaline phosphatase (AP), Gold nanoparticles (AuNPs), Antibody (Anti), Screen-printed carbon electrode (SPCE), Linear sweep voltammetry (LSV), Iron oxide nanoparticles (Fe<sub>3</sub>O<sub>4</sub>NPs), Differential pulse voltammetry (DPV), Electrochemical impedance spectroscopy (EIS), Screen printed electrode (SPE), Aptamer (APT), Streptavidin (SA), Graphene oxide (GO), Poly(3,4-ethylenedioxythiophene) (PEDOT), Fluorine tin oxide (FTO), Methylene blue-chitosan (MB-Chi), Graphene (GR), Indium tin oxide glass (ITO), Anthraquinone-2-carboxylic acid (AQ), Thionine chloride (TH), AgNO<sub>3</sub> (Ag<sup>+</sup>), Anti-mucin1 (anti-MUC1), Anti-cancer antigen 15-3 (anti-CA15-3), Anti-human epidermal growth factor receptor 2 (anti-HER2), Polyethylenimine (PEI), Square wave voltammetry (SWV).

## References

- 1 RCB, Marques., E, Costa-Rama., S, Viswanathan., HPA, Nouws., A, Costa-Garcia., C, Delerue-Matos., B, Gonzalez-Garcia., Voltammetric immunosensor for the simultaneous analysis of the breast cancer biomarkers CA 15-3 and HER2-ECD, *Sens. Actuators, B*, 2018, **255**, 918-925.
- 2 M, Emami., M, Shamsipur., R, Saber., and R, Irajirad., An electrochemical immunosensor for detection of a breast cancer biomarker based on antiHER2-iron oxide nanoparticle bioconjugates, *Analyst*, 2014, **139**, 2858-2866.
- 3 A, Florea., Z, Taleat., C, Cristea., M, Mazloum-Ardakani., and R, Sandulescu., Label free MUC1 aptasensors based on electrodeposition of gold nanoparticles on screen printed electrodes, *Electrochem. Commun.*, 2013, **33**, 127-130.
- 4 P, Gupta., A, Bharti., N, Kaur., S, Singh., and N, Prabhakar., An electrochemical aptasensor based on gold nanoparticles and graphene oxide doped poly(3,4-ethylenedioxythiophene) nanocomposite for detection of MUC1, *J. Electroanal. Chem.*, 2018, **813**, 102-108.
- 5 S, Cotchim., P, Thavarungkul., P, Kanatharana., and W, Limbut., Multiplexed label-free electrochemical immunosensor for breast cancer precision medicine, *Anal. Chim. Acta.*, 2020, **1130**, 60-71.

### **Calculation of % Decreasing Current**

The decreasing current percentage is measured before ( $I_0$ ) and after ( $I$ ) the immunoreaction between antibodies and antigens. The percentage of decreasing current is calculated as:

$$\% \text{ decreasing current} = \frac{(I_0 - I)}{I_0} \times 100$$